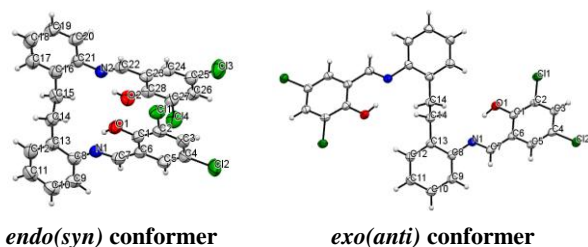# DFT Study on the Conformational Isomerism of Schiff base*N,N′*-bis(3,3′-dichlorosalicylidene)-2,2′-ethylenedianiline

Dong Seon Shin, Kil Sik Min, Bong Gon Kim

Abstract— **In previous work, we have isolated and characterized two conformers, *endo(syn)* and *exo(anti)* as Schiff base, *N,N′*-bis(3,5-dichlorosalicylidene)-2,2′-ethylenedianiline (L) containing the salicylidene and dianiline moieties. In this paper we have identified the conformational behavior of the Schiff base by DFT calculation using various methods as B3LYP, PBE1PBE, M06-2X, and M11L/6-311G(d,p) levels. And also we were investigated the mechanism of isomerism from the endo type conformer to the exo isomer by DFT calculation. The equilibrium geometries computed by all methods were compared with X-ray diffraction results. The conformational isomerism of the ligand were computed both in gas and in ethanol solution using PBE1PBE/6-311G(d,p).**

In the results of theoretical calculations, the Schiff-base ligand can be exist several conformational isomers according to torsion angle of main skeleton. We have identified that the more stable conformers are two conformers as endo01 and exo02 conformer. it was identified that The inter-conversion between two conformers can be easily achieved by thermo-control.

endo(syn) **conformer**   *exo(anti)* **conformer**

Index Terms-- **DFT, Schiff base, conformational isomerism, *N,N′*-bis(3,3′-dichlorosalicylidene)-2,2′-ethylenedianiline.**

I. INTRODUCTION

Schiff bases are important compounds bearing a general formula (R_1R_2)–C=N–R_3 with the characteristic carbon-nitrogen double bond which makes them be useful precursors for the synthesis of a variety of heteroatomic compounds. These compounds are usually synthesized by condensation of primary amines and active carbonyl groups. These compounds have attracted considerable attention due to their characteristic properties such as structural variety, varied coordinating ability, and thermal stability and potential applications as industrial, analytical and medicinal

Dong Sun Shin, Department of Chemistry Education, Gyeong sang National University, Jinju 660-701, Republic of Korea. Present address: Geoje Okpo High School, Teacher

Kil Sik, Min, Department of Chemistry Education, Kyungpook National University, Daegu 702-701, Republic of Korea.

Bong Gon, Kim, Department of Chemistry Education Gyeongsang National University, Jinju 660-701, Republic of Korea.

compounds [1-5]. Structural and spectroscopic investigations of pyridine–salicylaldehyde Schiff bases have been compared with theoretical DFT calculations [6]. Density Functional Theory (DFT) has been employed extensively to calculate variety of molecular properties e.g. equilibrium structure, charge distribution, UV–Vis and FT-IR spectra. It has provided reliable results which are in accordance with experimental data [7].

Our previous work, we have isolated and characterized two conformers, *endo* and *exo* as Schiff base, *N,N′*-bis (3,5-dichlorosalicylidene)-2,2′-ethylenedianiline containing the salicylidene and dianiline moieties.[8]. The aim of the present work is to present an investigation on the conformational isomerism of Schiff base, *N,N′*-bis (3,5-dichlorosalicylidene)-2,2′-ethylenedianiline (L) and explore the relationship of molecular structural parameters between experimental and calculated results by DFT. These quantum chemical parameters such as highest occupied molecular orbital energy (E_{HOMO}), lowest unoccupied molecular orbital energy (E_{LUMO}), energy gap (ΔE), the charge distributions, the absolute electro-negativity values (χ) , electron affinity ($A=- E_{LUMO}$), ionization potential ($I=-E_{HOMO}$), global hardness (η), softness (σ), and ionization potential (I) have been calculated. Meanwhile, according to structural parameters such as frontier orbital energy level, charge distribution and their interaction with metal ion, we could study on the reactivity indexes of Schiff bases.

II. COMPUTATIONAL DETAILS

We were interested in exploring the conformational stabilities, electronic structure and HOMO/LUMO make up of Schiff-base (1). For this purpose, the target Schiff base ligands have been studied geometry optimization. This procedure proceeded in two steps. Firstly, the initial geometry was conducted optimization using X-ray crystal structure of endo isomer (L1). Secondary, In order to explore conformational stabilities of the conformer, we have conducted the potential energy surface (PES) scan with variable torsion angles. The geometry of conformational isomer was fully optimized at the same level. At the optimized structure of the molecule, no imaginary frequency was obtained, proving that a local minimum of the PES was found.

The geometry optimization and harmonic vibration frequencies are performed by carrying out density functional theory (DFT) calculations with various methods (B3LYP, PBE1PBE, and M11L) [9-11] with a combination of 6-311G(d,p) basis set as implemented in Gaussian 09 suite of program [12]. GaussView 5.0.9 program is used for the visualization of the systems. The harmonic vibrational frequencies of the structures are calculated at the same level

to characterize their existence on the PES. The optimized structures are ensured by the absence of any imaginary frequency whereas any transition state is characterized by the presence of only one imaginary frequency.

III. RESULTS AND DISCUSSION

A. Stability of Conformational isomers

The Schiff base, *N,N′*-bis(3,5-dichlorosalicylidene)-2,2′-ethylenedianiline (L) can be formed several conformer according to torsion angles of main skeleton. Therefore, to investigate various conformational isomers, we have performed the DFT calculation of potential energy surface (PES) scanning as functions of torsion angles between the rings A and A'. The torsion angles of C8-C13-C14-C15 are varied in steps of 15˚ between 90 and -90 generating 26 points with fixed torsion angle C21-C16-C15-C14 using the geometry of *endo* type conformer. The results of PES are shown in *Figure* 1.
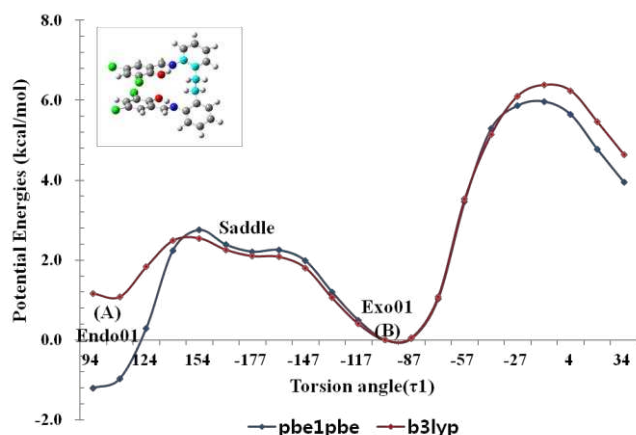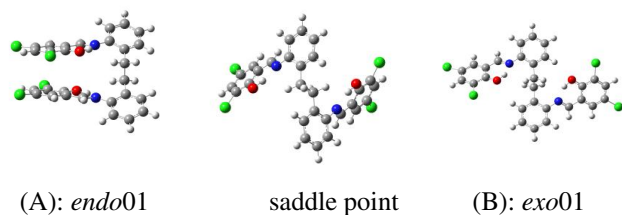

Figure 1. PES curves of *endo*- *N,N′*-bis(3,5-dichloro-salicylidene)-2,2′-ethylenedianiline obtained at DFT/6-311G (d,p) levels of theory: B3LYP(red). PBE1PBE (blue).

(A): *endo*01   saddle point   (B): *exo*01

As shown in *Figure* 1, we have found two local minima of conformers by PES scanning. Obtained conformer (B: *exo*01) was fully optimized at the above level. At the optimized structure of the molecule, no imaginary frequency was obtained, proving that a local minimum of the potential energy surface (PES) was found. But the geometry of conformer (B) is shown little different structure of the compound confirmed by X-ray crystallography.

In order to search a similar structure of the *exo*-type conformers (C: *exo*02), we have conducted the potential energy surface (PES) scan that the main chain torsion angle, C9-C8-N1-C7(D1) is varied in steps of 15˚ between 150˚ and -150˚ generating 26*26 points with fixed both torsion angles,

C21-C16-C15-C14(D2) and C8-C13-C14-C15(D3). The results of PES are shown in Figure S1 in SI. *Figure* 2 are shown typical feature of PES scanning.
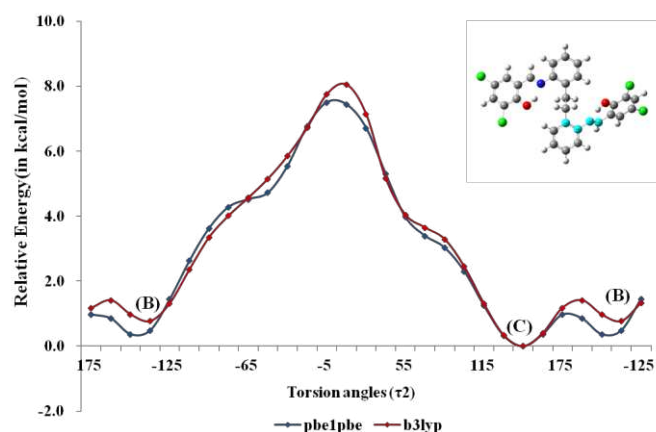
Figure 2. PES curves of *exo*-*N,N′*-bis(3,5-dichloro salicylidene)-2,2′-ethylenedianiline obtained at DFT/6-311G (d,p) levels of theory: B3LYP (red). PBE1PBE (blue).

(B) : exo01   (C) : exo02
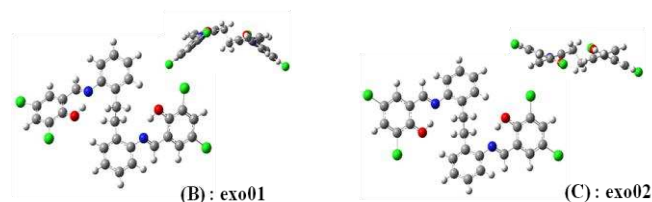
As shown in *Figure* 2, because of a low energy barrier in the reaction pathways, we can be seen that the conformational isomerism may occur easily the conformer (B) to conformer (C).The geometry of conformer (C) is very similar structure with the *exo*-conformer confirmed by X-ray crystallography. The geometries of typical conformers obtained from the various conditions via torsion angles are shown in *Figure* 3.

endo 01(Ⅰ)   *exo* 01(Ⅱ)

endo 02(Ⅲ)   *exo* 02(Ⅳ)
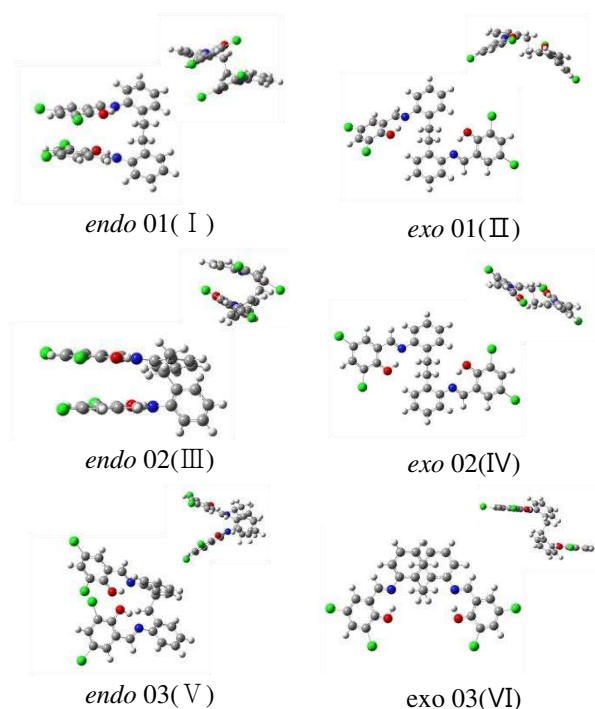
endo 03(Ⅴ)   exo 03(Ⅵ)

Figure 3. The geometries of typical conformers of *N,N′*-bis(3,5-dichlorosalicylidene)-2,2′-ethylenedianiline obtained at PBE1PBE /6-311G(d,p) levels of DFT theory.

Total energy(E_{Total}), Gibbs free energy($E_{\Delta G}$), Enthalpy ($E_{\Delta H}$), Entropy($E_{\Delta S}$), HOMO energy(E_{HOMO}), LUMO energy(E_{LUMO}) of various conformers at PBE1PBE/6-311G(d,p) level are given in Table 1.

Table 1. Relative energy, HOMO and LUMO energy of various conformers at PBE1PBE/6-311G(d,p) level

	I	II	III	IV	V	VI
TE[a]	0	0.31	3.33	0.06	2.45	2.89
ΔG[a]	0	-0.82	4.27	-1.07	1.00	0.25
ΔH[a]	0	0.31	3.33	-0.06	2.38	2.95
ΔS[a]	0	3.71	-3.41	3.46	4.68	8.88
LUMO	-0.083	-0.087	-0.085	-0.086	-0.082	-0.085
HOMO	-0.238	-0.242	-0.238	-0.242	-0.236	-0.242
E_g (eV)	4.20	4.22	4.25	4.15	4.43	4.25
η (eV)	2.10	2.11	2.12	2.07	2.22	2.13
χ(μ)	4.37	4.47	4.46	4.40	4.03	4.45

a: relative energy(kcal/mol)

As shown in Table 1, the total energies show that the *endo*01 and *exo*02 conformers are more stable than other conformers in gas phase. And also in all conformers, the total energies show that the enol form is more stable than keto form in gas phase. The values of torsion angles for the ligand suggest the planar nature of the six membered ring formed by the intramolecular hydrogen bond. The HOMO and LUMO energies of *exo* type conformers values become more negative than *endo* conformers. However, the extent of stabilization in HOMO energy is somewhat larger than that of LUMO energy, which results in an increased hardness value. The Gibbs free energies of conformers become to decrease in the following orders: III(*Exo*-02, -3177.6449) > II (*Exo*-01, -3177.6445) > I (*Endo*-01, -3177.6432) > VI(*Exo*-0 03, -3177.6428) > V (*Endo*-03, -3177.6416) > IV (*Endo*-02, -3177.6364) .

B. Conformational isomerism

In order to elucidate more detail description of conformational isomerism from *endo*(1) to *exo*(2), it was compared in the total energies and Gibbs free energies obtained by DFT calculation at each step. These results are shown in *Figure* 4.
Also, to elucidate the equilibrium relationship between *endo*-01 and *exo*-02 conformer, ΔG values obtained by DFT calculation were used to calculate equilibrium constants from the following formula:

$$\Delta G = -RT(\ln K)$$
$$\text{rate constant}, k = k_B T/hc^0 \exp\left(-\frac{\Delta^{\ddagger}G^0}{RT}\right)$$
$$K_C = \frac{k_f}{k_r}$$
$$Kc = \exp(-\Delta\Delta G^0/RT)$$

Here, R is the gas constant, T is temperature in Kelvin and assumed to be 298 in all calculations, and K is the equilibrium constant. The difference of Gibbs free energy and equilibrium constants which obtained from above equation in each step are shown in Table 2.
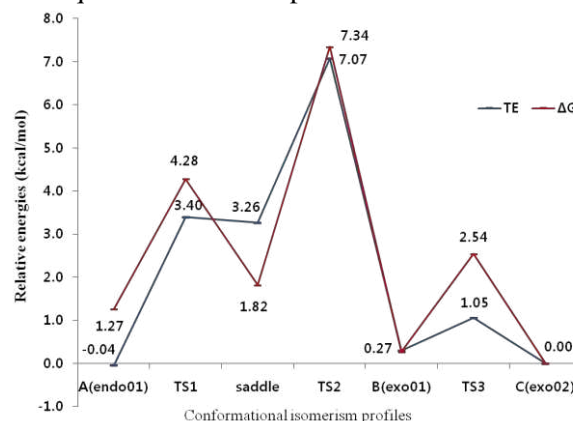

Figure 4. Reaction profiles of conformational isomerism from *endo* to *exo* conformer.

	Step 1	Step 2	Step 3	I to IV
ΔΔG⁰	0.555	-1.549	-0.277	-1.271
K_C	0.392	13.656	1.595	8.531

Generally, the low value of the total energy increases the stability of the isomers. It is known that the *endo*-01 conformers containing most negative total energy is more stable isomer among them.
On the other hand, it shows that the Gibbs free energy of the *exo*-02 isomer is the lowest value of among the isomers. In the second step, the higher energy barrier is shown that the conformational isomerism of the saddle form is more proceed to the *endo*-01 than to the *exo*-01 isomer at a relatively low temperature. However, in the third step, it can be seen that the conformational isomerism is very easily proceeds to the *exo*-02.
These results are indicated that the three conformational isomers may be existed at equilibrium state in gas phase. It can be seen that the higher energy barrier in second step relatively has not easy progressed to *exo*-01 isomer in the conformational isomerism in low temperature. Besides π in solid crystals is expected to add stability and easy pie is stacking the *exo*-02.

C. The structures of geometrical isomer

According to crystallographic data, the *endo* (L1)- and *exo* (L2)-type structures belong to monoclinic crystal systems with space groups of *C*2/*c* and *P*2₁/*c*, respectively. The molecular structure of the ligand was also investigated theoretically; see Scheme 1.The initial coordinates were obtained from the X-ray crystal structure determination and in the ground state (in vacuo) was optimized using DFT(B3LYP, PBE1PBE, M06-2X and M11L) with the 6-311G(d, p) basis sets. However, it should not be forgotten in here that the experimental results belong to solid phase and theoretical calculations belong to gaseous phase.
The optimized structures of *endo* and *exo* type conformers of *N,N′*-bis(3,5-dichlorosalicylidene)-2,2′-ethylenedianiline

from crystal data are comparable to theoretical data. The selected bond lengths and bond angles of *endo* and *exo* type Schiff base are given Table 2.

endo *exo*
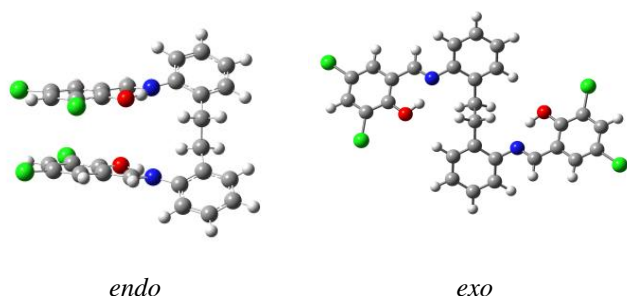
Scheme 1. The optimized geometries of *endo* and *exo* conformers obtained at DFT/PBE1PBE/6-311G(d,p) levels.

Table2. The selected bond lengths (Å), angles (◦) and torsion angles (◦) of endo and exo type Schiff bases in comparison with crystal data and theoretical data.

	Endo(1)			
	Exp.	b3lyp	Pbe1	M11L
	Bond lengths(Å)			
N1-C7	1.279(4)	1.286	1.283	1.273
N1-C8	1.427(4)	1.410	1.402	1.384
N2-C21	1.420(4)	1.410	1.402	1.382
N2-C22	1.275(4)	1.286	1.283	1.273
O1-C1	1.338(3)	1.332	1.323	1.307
C6-C7	1.448(4)	1.454	1.448	1.438
C13-C14	1.499(5)	1.512	1.503	1.436
	Bond angles(◦)			
C7-N1-C8	122.1(3)	121.64	121.30	120.52
C22-N2-C21	122.0(3)	121.64	121.30	120.81
O1-C1-C2	119.6(3)	119.76	119.93	118.99
O1-H-N1	147.56	148.99	150.05	147.63
O2-H-N2	146.65	148.99	150.05	147.60
N1-C7-C6	121.6(3)	122.03	121.72	122.14
C13-C8-N1	117.5(3)	119.02	118.93	118.76
N2-C22-C23	121.8(3)	122.03	121.72	122.03
O2-C28-C27	119.3(3)	119.77	119.93	118.92
O2-C28-C23	122.3(3)	122.23	122.19	123.32
	Dihedral angles(◦)			
C9-C8-N1-C7	25.5(5)	39.65	37.62	33.04
C20-C21-N2-C22	23.9(4)	39.66	37.62	32.84
C8-C13-C14-C15	97.0(4)	99.88	97.37	118.96
C21-C16-C15-C14	93.5(4)	99.91	97.30	77.38
C4-C26(pi=pi)		3.75	3.48	3.35

	Exo(1)			
	Exp.	b3lyp	Pbe1	M11L
	Bond lengths(Å)			
N1-C7	1.284(3)	1.286	1.283	1.272
N1-C8	1.420(3)	1.412	1.404	1.385
N2-C21				
N2-C22				
O1-C1	1.339(3)	1.333	1.323	1.306
C6-C7	1.462(3)	1.455	1.449	1.437

C13-C14	1.511(3)	1.513	1.505	1.492
	Bond angles(◦)			
C7-N1-C8 C22-N2-C21	120.2(2)	121.77	121.66	120.35
O1-C1-C2	120.0(2)	120.05	120.21	122.89
O1-H-N1 O2-H-N2	146.68	149.45	150.70	148.49
N1-C7-C6 C13-C8-N1	120.2(2)	121.77	121.66	120.35
N2-C22-C23	120.0(2)	120.05	120.21	122.89
O2-C28-C27 O2-C28-C23	146.68	149.45	150.70	148.49
	Dihedral angles(◦)			
C9-C8-N1-C7 C20-C21-N2-C22	-47.4(4)	-39.28	-38.14	-37.11
C8-C13-C14-C15 C21-C16-C15-C14 C4-C26(pi=pi)	-83.9(3)	89.24	87.69	85.14

For *endo* type conformer L1, the experimental bond lengths of N(1)-C(7), N(1)-C(8) and C(1)-O(1) are comparable with those of *enol* form obtained theoretically. For *exo* type conformer L2, the experimental bond lengths of N(1)-C(7), N(1)-C(8) and C(1)-O(1) are equivalent to those of *enol* form of optimized geometry. The small discrepancies between experimental and theoretical values are due to change in phase. Because crystal data correspond to structures in solid state, whereas calculated data correspond to structures in gas phase. And also single isolated molecule is considered in the DFT calculations, but the results of X-ray crystallography are associated with molecular packing.

The existence of hydrogen bonds in the optimized structures is observed in the N(1)-H-O(1) or N(2)-H-O(2) portion of *endo* type conformer and in the N(1)-H-O(1) portion of *exo* conformer, respectively. The O(donor)-H, H-N(acceptor) bond distances, and $\angle$ O-H-N bond angles are 1.000 Å, 1.664 Å, and 149.59˚, respectively. Whereas, the values obtained from X-ray crystallography are 0.84 Å, 1.858 Å, and 146.62˚, respectively. Similarly, for *exo* type conformer, the O-H, H-N bond distances, and $\angle$ O-H-N bond angles are 1.006 Å, 1.629 Å, and 150.57˚, respectively, and are comparable with X-ray data, 0.84 Å, 1.835 Å, and 146.69˚, respectively. Even though some differences are observed, in general, as shown in *Figure* 5, there are good matching between the calculated geometrical parameters and though obtained from X-ray structure.

Plotting experimental values vs calculated values of structural parameters demonstrate a good relationship between both parameters. The linear relationship is clearly demonstrated, as a linear regression yields R^2 of *endo* isomer (1) are 0.958, 0.949, and 0.980 for bond lengths, 0.956, 0.956, and 0.939 for bond angles, 0.998, 0.997, and 0.990 for torsion angles by optimized methods in B3LYP, PBE1PBE, and M11L, respectively. And also R^2 of *exo* isomer (L2) are 0.951, 0.940, and 0.952 for bond lengths, 0.963, 0.963, and 0.984 for bond angles, 0.999, 0.999, and 0.999 for torsion angles by optimized methods in B3LYP, PBE1PBE, and M11L, respectively. All calculated structural parameters are
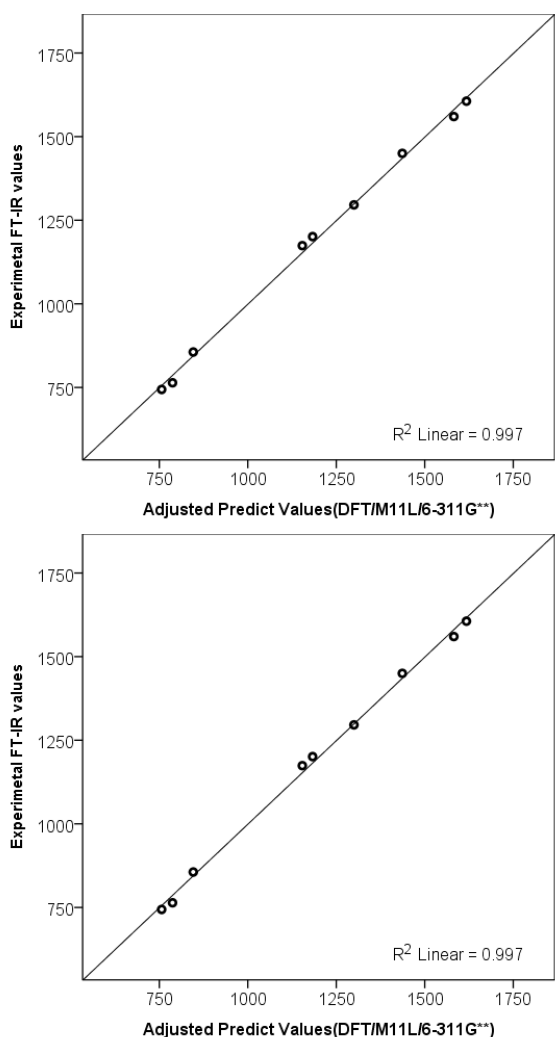
in good agreements with experimental values in all the methods.

Figure 5. Plot of relationship for bond lengths between experimental values by X-ray crystallography vs. calculated values by DFT in *endo*(upper) and *exo*(down) conformers.

D. FT-IR spectra of geometrical isomer

Figures 7-8 show the FT-IR and computed IR frequencies of tautomers of two conformer calculated by M11L and PBE1PBE/6-311G(d,p) methods. The experimentally observed band at 3400 cm^{-1} corresponds to phenolic O-H stretching frequency. The stretching frequency observed broad band shows the presence of O-H···N intra-molecular hydrogen bonding in the compounds. Generally, very intensive band in the 1660-1500cm^{-1} region is diagnostic of the IR spectra of Schiff base.

For the title compounds, this band is appeared at 1616, 1614 cm^{-1}, respectively, which is related to the stretching modes of the C=N bonds. However, this mode is strongly coupled with C=C stretching vibrational modes of title compounds, the calculated mode with M11L/6-311(d,p) are 1696(*endo* 01), 1695 (*exo* 02)cm^{-1}, respectively. The appearance of the phenolic C-O band around 1516 cm^{-1} and disappearance of the NH bands are evidence of the existence of *enol* form in the solid state.

Figure 6. Experimental and calculated IR spectra of *endo* type conformer. (A) pbe1pbe//*enol*(COH···N); (B) *keto*(CO···HN) (C) M11L//*enol*(COH···N); (D): Experimental data

enol, OH   keto, NH

Figure 7. Experimental and calculated IR spectra of *exo* type conformer. (A) pbe1pbe/*enol*(COH···N); (B) *keto*(CO···HN) (C): M11L//*enol*(COH···N); (D) Experimental data

Compared with the experimental values, DFT calculated values some overestimates the frequencies. As shown *Figure* 8, plotting experimental values vs calculated values of IR frequencies demonstrate a good relationship between both parameters. The linear relationship is clearly demonstrated, as a linear regression yields R^2 of *enol* type *endo*(L1) conformer are 0.998. And also R^2 of *enol* type *exo* isomer(L2) are 0.997. The calculated vibrational frequencies of enol type are in good agreement with experimental ones.

Figure 8. Plot of relationship for selected vibrational frequencies between experimental values by FT-IR spectrum vs. calculated values by DFT in *endo*(upper) and *exo*(down) type conformer.

IV. CONCLUSIONS

In this paper we have identified the conformational behavior of the Schiff base by DFT calculation using various methods as B3LYP, PBE1PBE, M06-2X, and M11L/6-311G(d,p) level of theory and investigated the mechanism of isomerism from the endo type conformer to the exo isomer by DFT calculation. The equilibrium geometries computed by all methods were compared with X-ray diffraction results. The conformational isomerism of the ligand were computed both in gas and in ethanol solution using PBE1PBE/6-311G(d,p). In the results of theoretical calculations, the Schiff-base ligand can be exist several conformational isomers according to torsion angle of main skeleton. we have identified that the more stable conformers are two conformers as *endo*01 and *exo*02 conformer. it was identified that The inter-conversion between two conformers can be easily achieved by thermo-control.

REFERENCES

[1] Refat M.S., El-Sayed M.Y., Adam A.M., J. Mol. Struct. 1038 (2013) 62–72.

[2] Hormnirun P., Marshall E. L., Gibson V. C., Pugh R. I., and White A. J. P. PNAS 103 (2006),42, 15343-15348

[3] Sarkar S., Lee W. R., Hong C. S., Lee H.IBull. Korean Chem. Soc., 34, .(2013) 2731-2736

[4] S. Yamada, Coord. Chem. Rev. 192 (1999) 537.

[5] Ferraresi-Curotto V., Echeverría G.A., Piro O. E., Pis-Diez R., González-Baró C., Spectrochimica Acta Part A, 137, (2015) 692-700.

[6] Miyasaka] H., Saitoh A., Abe S., Coord. Chem. Rev. 251 (2007) 2622–2664.

[7] Hwang K.Y., Kim H., Lee Y.S., Lee M.H., and Do YChem. Eur. J., 15, .(2009) 6478-6487

[8] Min K.S., Kim Y.J., Ko H.J., Kwak D.H., Kim T.W., Shin J.W., Kim B.G., J. Phy. Org. Chem.(2014), 27, 960-966.

[9] Annaraj B., Pan S., Neelakantan M.A., Chattaraj P. K. Computational and Theoretical Chemistry 1028 (2014) 19–26.

[10] a) Lee C., Yang W., Parr R.G, Phys. Rev. B 37 (1988) 785–789. b) Perdew J.P, Burke K., Wang Y, Phys. Rev. B 54 (1996) 16533–16539.

[11] Castro A, Marques M.A.L., Alonso J.A., Bertsch G.F., Rubio A., Eur. Phys. J., D28 (2004) 211-218.

[12] Frisch M. J., G. W. Trucks, H. B. Schlegel, G. E. Scuseria, M. A. Robb, J. R. Cheeseman, G. Scalmani, V. Barone, B. Mennucci, G. A. Petersson, H. Nakatsuji, M. Caricato, X. Li, H. P. Hratchian, A. F. Izmaylov, J. loino, G. Zheng, J. L. Sonnenberg, M. Hada, M. Ehara, K. Toyota, R. Fukuda, J. Hasegawa, M. Ishida, T. Nakajima, Y. Honda, O. Kitao, H. Nakai, T. Vreven, J. A. Montgomery, Jr., J. E. Peralta, F. Ogliaro, M. Bearpark, J. J. Heyd, E. Brothers, K. N. Kudin, V. N. Staroverov, R. Kobayashi, J. Normand, K. Raghavachari, A. Rendell, J. C. Burant, S. S. Iyengar, J. Tomasi, M. Cossi, N. Rega, N. J. Millam, M. Klene, J. E. Knox, J. B. Cross, V. Bakken, C. Adamo, J. Jaramillo, R. Gomperts, R. E. Stratmann, O. Yazyev, A. J. Austin, R. Cammi, C. Pomelli, J. W. Ochterski, R. L. Martin, K. Morokuma, V. G. Zakrzewski, G. A. Voth, P. Salvador, J. J. Dannenberg, S. Dapprich, A. D. Daniels, O. Farkas, J. B. Foresman, J. V. Ortiz, J. Cioslowski, D. J. Fox, Gaussian 09, Revision A.1; Gaussian, Inc.: Wallingford CT (2009).